A THEORETICAL CONTRIBUTION TO THE PROBLEM OF TOWPLANE UPSET

by Guido de Matteis, Department of Aerospace Engineering, Polytechnic of Turin, Turin, Italy

Presented at the XXV OSTIV Congress, Saint Auban, France

Summary

The effect of design and operating parameters on towplane upset is investigated by numerical simulation of the coupled system represented by towplane, towrope and sailplane. The relevant role played by tow-hook location, rope length and tow speed on the perturbated motion of the complete system is analyzed and discussed.

1. Introduction

In this study a full dynamic model of the towplane, cable and sailplane system is used to investigate the effect of design and operating parameters on the so-called towplane upset phenomenon. The scenario of this kind of accident involves an initial upward displacement of the sailplane as it acquires a higher position behind the tug. The towplane is forced to pitch sharply nose-down due to the negative pitching moment caused by the rope tension and, as a result, the velocity of the two vehicles significantly increases. It is to be noted that a nose-up pitching tendency of the sailplane is particularly hazardous at low speed during the early stages of the launch when the height is too low for the towplane to recover. In fatal accidents the aforementioned situations are reported to occur so rapidly that pilots are unable to release.

As a result of accident investigations, the initial displacement of the glider was explained as due to (i) air turbulence including thermals, hill or wave rotors, (ii) hurried corrections made by the sailplane pilot in climbing when, due to a marked wind gradient, the glider acquires a lower position with respect to the tug. In fact, an upward position of the sailplane during aerotowing drives the system into a dynamically unstable situation, as shown in Refs. 1, 2, and therefore such a vertical displacement appears to be the critical circumstance which initiates the sequence of events leading to the upset.

Following a number of fatal accidents occurring to towplane pilots during aerotow, which were explained as due to the sailplane pitching up in an apparently uncontrolled mode, the fitting of a nose- or forward hook was proposed in the JAR 22 requirements (Notice of Proposed Amendment NPA 22D-35) as a design change to sailplanes approved for aerotowing. In particular, it was recognized that a tow hook located on centre of gravity (c.g.) can produce pitch divergency and loss of control. In this respect, it was shown in previous researches[1,2,3] that the

Nomenclature

A	rope cross section
b	wing span
C_{Dc}, C_{Lc}	aerodynamic coefficients of the rope
C_{Do}, k	force coefficients of the rope
d	rope diameter
E	Young's modulus
$I\eta$	moment of inertia, about η
$\mathbf{F}$	aerodynamic force
F_I, F_V, F_W	inertial, body and wind reference frame, respectively
$\mathbf{g}$	acceleration of gravity
$\mathbf{I}$	inertia matrix
l	length of the rope
$\mathbf{L}_{VI}$	transformation matrix from F_I to F_V
$\mathbf{L}_{WV}$	transformation matrix from F_V to F_W
$\mathbf{M}$	aerodynamic moment
m	mass
$\mathbf{n}$	load factor
$\mathbf{P}$	position vector in F_I
$\mathbf{R}_a$	$= (\xi_a, 0, \zeta_a)^T$ position vector of the attachment point in F_V
s	curvilinear abscissa
$\mathbf{T}$	thrust force
t	time
$\mathbf{t}$	$= (\partial x/\partial s, \partial y/\partial s, \partial z/\partial s)^T$ unit vector tangent to the rope in F_I
U_e	reference velocity
$\mathbf{v}_c$	$= (U_c, V_c, W_c)^T$ local velocity vector of the rope in F_I
$\mathbf{v}_G$	$= (U_G, V_G, W_G)^T$ c.g. velocity in F_I
$\mathbf{v}_{rc}$	$= -(U_e + U_c, V_c, W_c)^T$ local rope velocity relative to the fluid in F_I
$\mathbf{v}_r$	$= -\mathbf{L}_{VI}(U_e + U_G, V_G, W_G)^T$ aircraft velocity relative to the air in F_V
x, y, z	coordinates in inertial axes

Greek symbols

α	angle of attack
γ	flight path angle
δ_E	elevator angle
ϵ	stretching
v	rope mass per unit length
ξ, η, ζ	coordinates in body axes
ρ	density
τ	tension force
Φ	$= (\phi, \theta, \psi)^T$ Euler angle vector

Subscripts

A	tow-plane
a	attachment point
B	sailplane
c	cable
e	equilibrium
G	center of mass
r	relative
0	unstretched

static stability of the sailplane is increased as the hook position is moved forward.

By recognizing that the requirement of a nose-hook was only a partial solution and in order to minimize the risk of towplane upset, in 1993 the JAR-22 Study Group issued the NPA 22B-49 that introduced the requirement for manufacturers to demonstrate that the sailplane is safely controllable in aerotowing during critical combinations of a number of conditions, namely tow rope length and inclination, flap and trim setting, longitudinal acceleration, and average pilot skill. As for the reported reasons for the strong opposition to the NPA's from the designers, we only mention here the high cost of installation of the nose-hook together with the poor evidence of its effectiveness in reducing the upset occurrence, and the absence of any criteria for flight testing in circumstances which can bring the towplane in a very dangerous flight attitude. To the author's knowledge, the cited NPA's have not taken the form of specification so far.

In such a context, the application of a three-dimensional, nonlinear model to the simulation of the system motion following assigned control inputs can provide a relevant contribution to the analysis of towplane upsets. In the analysis of the phenomenon the influence of several parameters on the stability of the two aircraft is to be carefully explained and quantified and, to this end, adequate flight testing is not an option for both safety reasons and the high cost of the equipment necessary for data acquisition.

In the mathematical model we have three coupled sets of equations related to the cable, the towplane and the glider. The initial equilibrium configuration corresponds to a steady flight at constant altitude of the two vehicles. Included in the model are the towplane and sailplane inertial and aerodynamic characteristics and, as far as the cable is concerned, its mass, length, elastic modulus and aerodynamic coefficients. Former applications of the present model were in the stability analysis[2] of the complete system, and in the study of the sensitivity of the longitudinal and transversal characteristic modes to changes of design and operating data,[3] in order to identify which parameters influence the system dynamics and which ones do not.

Following the debate recalled earlier on the possible means of preventing upward departures of the sailplane, we use numerical simulation to quantatively assess the influence of certain factors on towplane upsets. In particular, by determining the response of the coupled system to inputs on the glider elevator we analyze the effect of hook location as a design parameter and the influence of tow speed, and cable length and elasticity as operating parameters.

In the sequel, the mathematical model of the two aircraft and the rope, and the procedure of integration of the governing equations are briefly recalled in Section 2. The upsets are simulated by computing the time histories of significant states, and the results of the analysis are presented and discussed in Section 3. A section of conclusions ends the paper.

2. Mathematical model

In what follows the principal aspects of the mathematical model of the towplane-cable-sailplane system sketched in Figure 1, are reported in concise form. Reference is made to References 2 and 3 for further details on the formulation of the governing equations.

The towplane (A) and the sailplane (B) are modelled as rigid bodies and the pertinent equations of motion in vector form are written, in body axes $F_V(\xi,\eta,\zeta)$, as[4]

$$m_A \mathbf{L}_{VI_A} \dot{\mathbf{v}}_{G_A} = \mathbf{F}_A + \boldsymbol{\tau}_{a_A} + m_A \mathbf{L}_{VI_A} \mathbf{g} + \mathbf{T} \quad (1)$$

$$m_B \mathbf{L}_{VI_B} \dot{\mathbf{v}}_{G_B} = \mathbf{F}_B - \boldsymbol{\tau}_{a_B} + m_B \mathbf{L}_{VI_B} \mathbf{g} \quad (2)$$

and

$$\mathbf{I}_A \dot{\boldsymbol{\omega}}_A + [\boldsymbol{\omega} \times (\mathbf{I}\boldsymbol{\omega})]_A = -(\boldsymbol{\tau}_a \times \mathbf{R}_a)_A + \mathbf{M}_A \quad (3)$$

$$\mathbf{I}_B \dot{\boldsymbol{\omega}}_B + [\boldsymbol{\omega} \times (\mathbf{I}\boldsymbol{\omega})]_B = (\boldsymbol{\tau}_a \times \mathbf{R}_a)_B + \mathbf{M}_B \quad (4)$$

where the c.g. velocity $\mathbf{v}_G$ is in an inertial reference system $F_I(x,y,z)$ the origin of which coincides with the c.g. of the towplane in the reference condition of steady, level and symmetric flight. It has to be remarked that the origin of F_I moves at the reference speed U_e with respect to a flat Earth-fixed reference frame. In Eqs. (1)-(4), $\boldsymbol{\tau}_{aA,B} = (|\boldsymbol{\tau}| \mathbf{L}_{VI}\mathbf{t})_{aA,B}$ indicates the tension force in the attachment points $a_{A,B}$ of the rope, $|\boldsymbol{\tau}| = \epsilon AE$ is the tension force modulus, and the meaning of the other symbols is reported in the Nomenclature. In the expression of the aerodynamic force (**F**) and moment (**M**), the relative velocity of the aircraft with respect to the air ($\mathbf{v}_r$) is used.

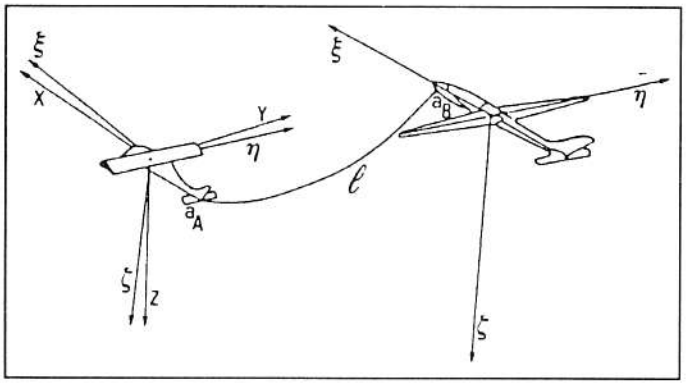

Figure 1. Sketch of the system.

The rope is modelled as a continuous, elastic and perfectly flexible one-dimensional body, subjected to distributed aerodynamic and mass forces according to the equation[5]

$$\nu \frac{\partial \mathbf{v}_c}{\partial t} = \frac{\partial}{\partial s}(|\boldsymbol{\tau}|\,\mathbf{t}) + \nu \mathbf{g} + \frac{1}{2}\rho d\,[C_{L_c}\mathbf{v}_{r_c} \times (\mathbf{v}_{r_c} \times \mathbf{t}) + C_{D_c}|\mathbf{v}_{r_c}|\mathbf{v}_{r_c}] \quad (5)$$

The stretching ϵ is expressed as

$$\epsilon = \left[\left(\frac{\partial x}{\partial s_0}\right)^2 + \left(\frac{\partial y}{\partial s_0}\right)^2 + \left(\frac{\partial z}{\partial s_0}\right)^2\right]^{1/2} - 1 \quad (6)$$

where the subscript 0 indicates unstretched. For the lift and drag coefficient of the rope we write[5]

$$C_{L_c} = k(1 - \cos^2 \alpha_c) \cos \alpha_c$$

$$C_{D_c} = C_{D_0} + k(1 - \cos^2 \alpha_c)^{3/2} \tag{7}$$

with $\cos \alpha_c = \mathbf{v}_{rc} \cdot \mathbf{t} / |\mathbf{v}_{rc}|$.

The three sets of fundamental equations, namely Eqs. (1)-(4) for the aircraft and Eq. (5) for the rope, are coupled when we express the boundary conditions at the two ends of the rope by kinematic relations in terms of position and speed of the two vehicles

$$\frac{d\mathbf{P}_{a_A}}{dt} = \mathbf{v}_{G_A} + [\mathbf{L}_{IV}(\boldsymbol{\omega} \times \mathbf{R}_a)]_A \tag{8}$$

$$\frac{d\mathbf{P}_{a_B}}{dt} = \mathbf{v}_{G_B} + [\mathbf{L}_{IV}(\boldsymbol{\omega} \times \mathbf{R}_a)]_B \tag{9}$$

where the rope coordinates at the attachment point $\mathbf{P}_{aA,B}$ are in $F_I(x, y, z)$. In order to complete the set of governing equations we have the following relations for $\mathbf{P}_c(s)$, $0 < s < 1$

$$\frac{\partial \mathbf{P}_c}{\partial t}(s) = \mathbf{v}_c(s) \tag{10}$$

and for the Euler angle rates

$$\dot{\boldsymbol{\Phi}}_{A,B} = \mathbf{R}^{-1}_{A,B} \boldsymbol{\omega}_{A,B} \tag{11}$$

where $\mathbf{R}^{-1}$ is a transformation matrix.[4]
Finally, the load factor of the glider $\mathbf{n}_B$, in wind axes F_W, is expressed as

$$\mathbf{n}_B = \left(\mathbf{L}_{WV} \frac{\boldsymbol{\tau}_a - \mathbf{F}}{m\,|\mathbf{g}|} \right)_B \tag{12}$$

As a comment on the system model we observe that the aerodynamic interference between the towplane and the sailplane, and the effects of unsteady aerodynamics are all neglected. Also, nonlinear extensional stiffness and torsional stiffness of the rope are not taken into consideration. Finally, very low tension conditions, i.e. $\tau \leq 5$-10 N, can not be simulated since, in such circumstances, an appropriate model of the stress-strain behavior as the tension of the rope approaches zero, would be necessary.

Partial derivatives in Eqs. (5) and (6) are made discrete in space by a modified differential quadrature method[6], and the resulting set of governing equations is numerically integrated in time by a fourth-order Runge-Kutta routine. As for the determination of the reference condition, we assign the flight speed U_e and the angle of attack of the glider α_{Be}. Then, the nonlinear set of algebric equations corresponding to Eqs. (1)-(11) written in steady-state, is solved by an iterative procedure,[2] and the cable shape, c.g. coordinates, attitude and control angles for the two vehicles are determined. The distance Δz between sailplane and towplane c.g.'s is also evaluated. In this study we consider symmetric flight in both steady-states and perturbed motions.

3. Results and discussion

In the simulations we use models of a Cessna 172[7] type towplane and a M-100 S[8] sailplane. In particular, for the tug we have $m_A = 800$ kg, $I_{\eta A} = 1{,}800$ kgm^2 and $b_A = 11$ m, whereas the glider has $m_B = 300$ kg, $I_{\eta B} = 200$ kgm^2 and $b_B = 15$ m. The towrope data are $d = 0.011$ m, $EA = 3.61 \times 10^4$ N and $v = 8.3 \times 10^{-2}$ kgm^{-1}. The hook location in the towplane is at $\xi_{aA} = -4.9$ m and $\zeta_{aA} = 0.25$ m, where ξ_{aA} and ζ_{aA} are the hook coordinates in the body-fixed reference frame (Figure 1). As we said earlier, the initial condition at $t = 0$ for the simulations is a steady horizontal flight at sea level. Note that the vertical separation of the aircraft Δz is assigned when we select a value for the angle of attack α_{Be} of the glider. In this application no constraints on the cable shape are enforced, as for instance a maximum value of tow-angle related to the configuration of the tail surfaces of the tug.

Figures (2)-(5) illustrate the results of the simulations when the effects of hook position and rope length are investigated. In the figures the time histories of nondimensional perturbation velocity $|\mathbf{V}_G|_B / U_e$, glide angle γ, angle of attack relative to steady-state $\alpha - \alpha_e$, normal load factor for the sailplane n_B and tension force at the sailplane hook $|\tau_a|_B$ are shown for a time length of 6.3 s. The towspeed at the initial time is $U_e = 30$ ms^{-1} and the system is perturbed by a step, pitch-up input $\Delta\delta_{EB} = -1$ deg on the glider elevator that occurs at $t = 1$ s. In all the computations we have $|\Delta z| < 1$ m at $t = 0$. We observe in all the reported cases that the sailplane speed is initially decreased whereas the glide angle is increased by the control action. As a result the glider climbs up to a higher position with respect to the tug. Then the towplane rotates nose-down because of the rope tension at the aft hook, and its path angle sharply decreases together with the angle of attack. This behavior is further revealed when the cable shape at different times is considered, as reported in Figures. 6.a and 6.b for a towrope length of 40 and 60 m, and c.g. ($\xi_{aB} = 0.52$, $\zeta_{aB} = 0.58$ m) and nose-hook ($\xi_{aB} = 1.74$, $\zeta_{aB} = 0.42$ m) position, respectively. Note that in order to report the perturbated configuration of the rope, its coordinates, made nondimensional with respect to the unstretched rope length, are presented in the frame F_I that moves at constant speed U_e.

As for the effect of the rope length, we compare Figures 2 and 3 to Figures 4 and 5, respectively. In both cases of c.g. and nose-hook the longer rope produces a slower divergence of the reported states. The influence of the hook position is also relevant and, in this respect, Figures 2 and 4 are to be compared to Figures 3 and 5, respectively. For a given length of the rope the system appears more controllable when the hook is in the forward location. As an example, for $l_0 = 40$ and nose-hook, the tension force on the sailplane at $t = 5.3$ s, is reduced to a value of 2400 N with respect to the value of 5100 N obtained, at the same time, by using the c.g. hook. This kind of behavior of the system is to be related to a positive effect of the towing action on the static stability of the glider since the tension force, when applied in a forward position with respect to the c.g., gives

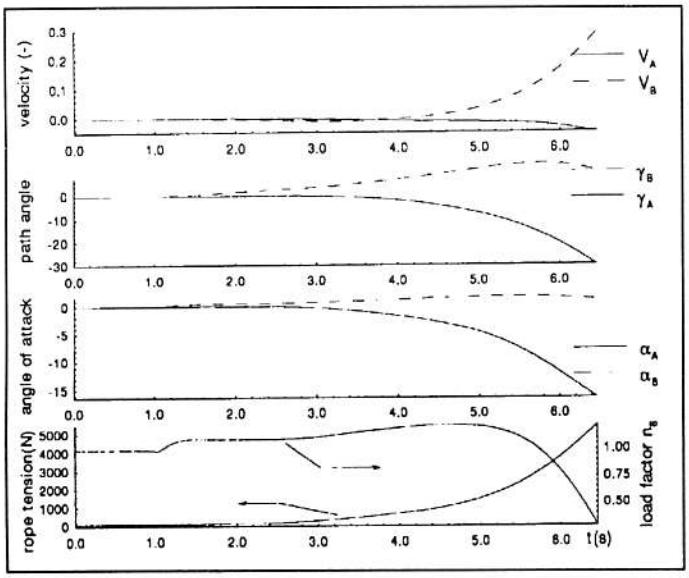

Figure 2. Time history of the system $\Delta\delta_{EB}$ = -1 deg, U_e = 30 ms,$^{-1}$ c.g. hook, l_0 = 40 m.

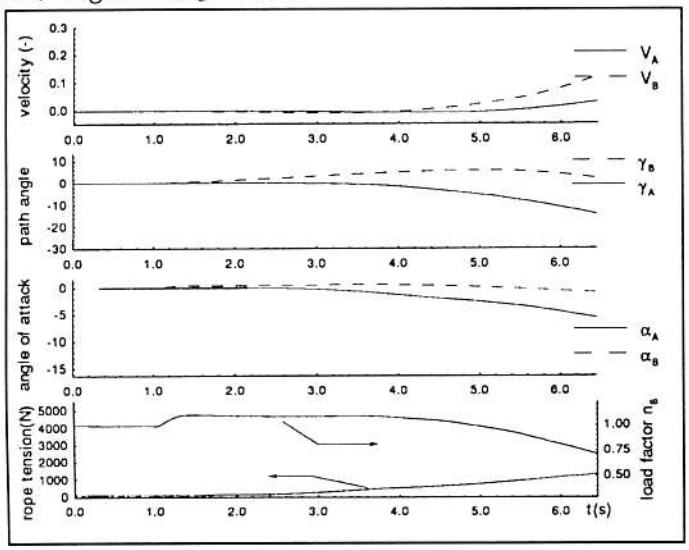

Figure 3. Time history of the system $\Delta\delta_{EB}$ = -1 deg, U_e = 30 ms,$^{-1}$ nose hook, l_0 = 40 m

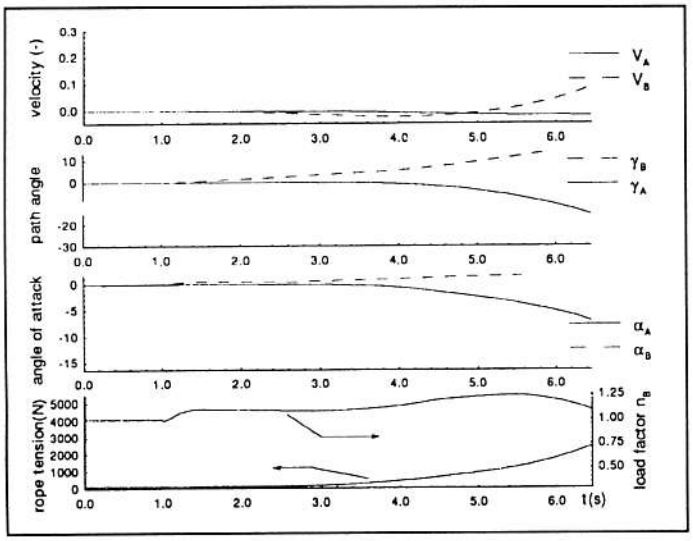

Figure 4. Time history of the system $\Delta\delta_{EB}$ = -1 deg, U_e = 30 ms,$^{-1}$ c.g. hook, l_0 = 60 m.

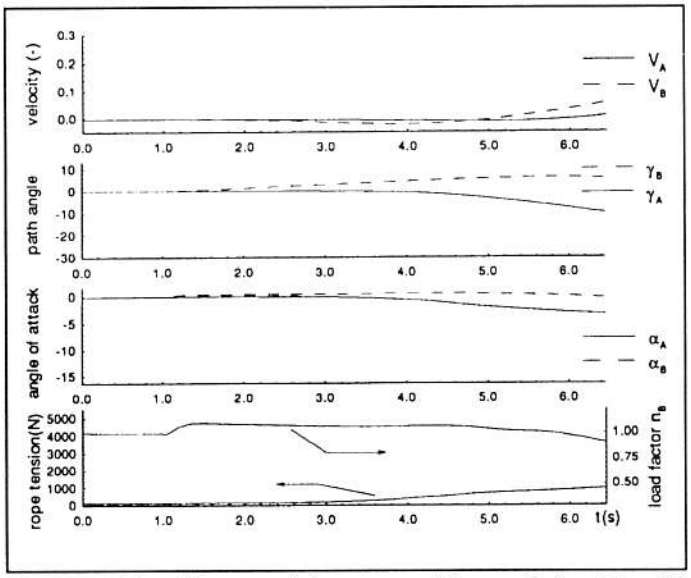

Figure 5. Time history of the system $\Delta\delta_{EB}$ = -1 deg, U_e = 30 ms,$^{-1}$ nose-hook, l_0 = 60 m.

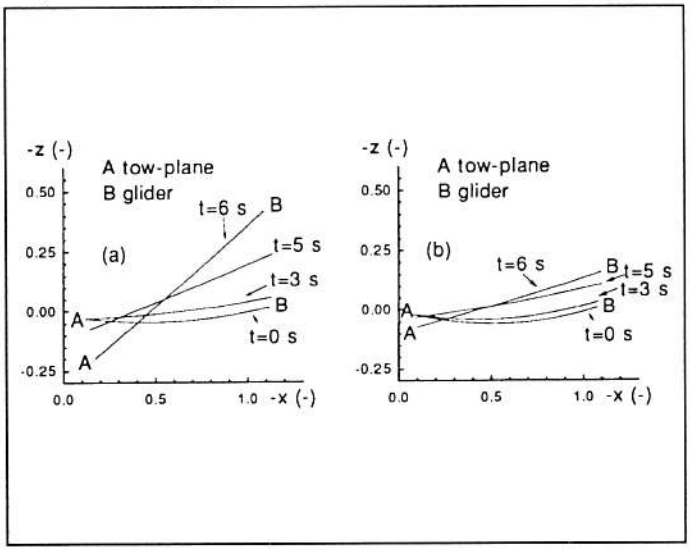

Figure 6. Rope shape and position at different times, U_e = 30 ms^{-1}: (a) c.g. hook, l_0 = 40 m, (b) nose-hook, l_0 = 60 m.

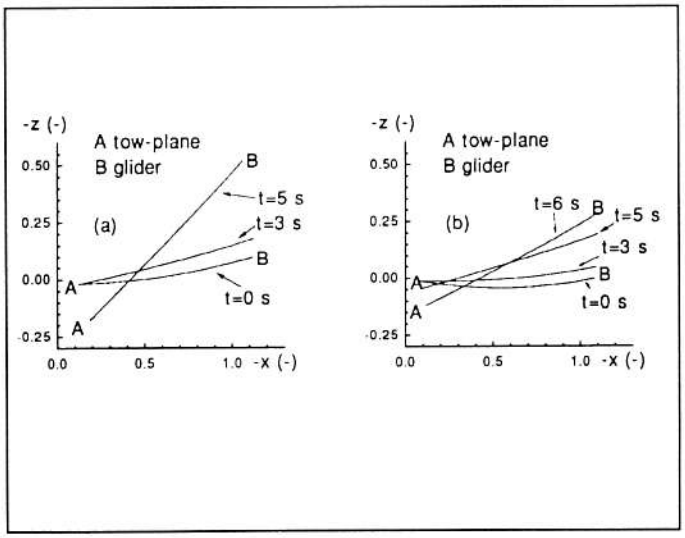

Figure 7. Rope shape and position at different times, U_e = 40 ms^{-1}: (a) c.g. hook, l_0 = 40 m, (b) nose-hook, l_0 = 60 m.

Table 1. Velocity ratio a $t = 6$ s.

$\lvert v_r \rvert_B / U_e$	hook position	l_0
1.065	nose	40
1.030	nose	60
1.170	c.g.	40
1.045	c.g.	60

a stabilizing contribution to the restoring, pitch-down moment caused by an increase of the angle of attack. Note in all the figures that n_B is reduced at the end of the simulation since the glider is forced to push-down by the rope tension.

In Figure 6 the significant differences in the state evolution due to the considered parameters can be observed in terms of rope shape and aircraft position in two circumstances, namely c.g. hook, $l_0 = 40$ m (Figure 6.a) and nose-hook, $l_0 = 60$ m (Figure 6.b), respectively.

Finally, in order to provide quantitative information on the system tendency to diverge due to the nose-up elevator command, Table 1 shows the velocity ratio $\lvert v_r \rvert_B / U_e$ at $t = 6$ s for the considered configurations. The results discussed earlier from a qualitative point of view are now substantiated as we note that, by using a longer rope, we can reduce to a certain extent the negative effect of an aft hook location on the system stability.

The effect of tow speed is illustrated in Figure 7, where the rope shape is reported as a function of time for the two situations already analyzed in Figure 6 at a tow speed of 30 ms^{-1}. The reference speed is now $U_e = 40$ ms^{-1} and we have a 1.9 degree decrease of α_{Be} in order to realize the same relative position of the aircraft as in the previous cases. The increased velocity causes larger perturbations on the motion variables and, as a result, the system displacement from the reference condition is enhanced. In this respect, note that the simulation of the configuration with $l_0 = 40$ m and c.g. hook was terminated at $t = 5.3$ s due to a rope tension as high as 8000 N and a sailplane velocity $\lvert V_G \rvert_B / U_e = 1$.

As a final result, some simulations were run at different values of the elastic modulus of the rope. In particular, for $E = 5 \times 10^8, 1 \times 10^9, 1.5 \times 10^{10}$ Nm^{-2} we obtain for the velocity ratio defined above, values of 1.037, 1.036 and 1.030, respectively. Therefore, it is apparent that the system response is slightly affected by this parameter, at least in the considered range of variation. In this respect we observe that in previous studies,[2,3] apart from its influence on the elastic behavior of the rope, the elastic modulus was shown to have a relevant effect on the stability of the complete system.

4. Conclusions

In this study the influence of design and operating parameters on the sequence of events leading to a diverging motion of a towed sailplane has been investigated by computer simulation. The system response to control inputs on the glider elevator has been determined and, as a result, the effects of cable length and elastic modulus, tow speed and tow hook location have been analyzed. It is apparent that the stability of the system in the considered flight conditions is enhanced by (i) a forward position of the towing hook because the restoring pitching moment is increased and (ii) a longer cable and/or a reduced speed since in these circumstances the time constant of the perturbed motion is larger.

As possible further development and applications of the presented mathematical model of the sailplane in towed flight we would cite the analysis of flight in a turbulent atmosphere and in wind gradients, the study of piloted flight when a model of the sailplane pilot is implemented in the system and, finally, the simulation of controlled maneuvers in three-dimensional flight phases.

Acknowledgments

The author thanks Prof. P. Morelli of the Polythecnic of Turin for his interest and helpful advice in this work.

References

1. Maryniac, J., "Simplified Longitudinal Stability of a Towed Sailplane," *Mechanica Teoretyczna i Stozowana*. Vol. 5, No. 1, 1967, pp. 57-101.
2. de Matteis, G., "Longitudinal Dynamics of a Towed Sailplane," *Journal of Guidance, Control and Dynamics*, Vol. 16, No. 5, 1993, pp. 812-819.
3. de Matteis, G., de Socio, L.M., "A Sensitivity Analysis of the Stability of a Tug-Rope-Sailplane System," Proc. of the 18th ICAS Congress, Beijing, China, 1992, pp. 2016-2023.
4. Etkin, B., *Dynamics of Atmospheric Flight*, John Wiley and Sons, Inc., New York, 1972, Chapt. 4.
5. De Laurier, J.D., "A First Order Theory for Predicting the Stability of Cable Towed and Tethered Bodies where the Cable has a General Curvature and Tension Variation," von Karman Institute Technical Note 68, Rhode-Saint-Geneve, Belgium, Dec. 1970.
6. Satofilka, N., A New Explicit Method for the Numerical Solutions of Parabolic Differential Equations," *Numerical Properties and Methodologies in Heat Transfer*, edited by T.M. Shih, Hemisphere, Washington, D.C., 1983, pp. 97 108.
7. Roskam, J., *Airplane Flight Dynamics and Automatic Flight Control*, Roskam Aviation and Engineering Corporation, Ottawa, Kansas, 1979.
8. Morelli, P., *Static Stability and Control of Sailplanes*, O.S.T.I.V., Voorburg, The Netherlands, 1976.